JACS
JOURNAL OF THE AMERICAN CHEMICAL SOCIETY
pubs.acs.org/JACS
Article

Measuring Aptamer Folding Energy Using a Molecular Clamp

Hao Qu,* Qihui Ma, Lu Wang, Yu Mao, Michael Eisenstein, Hyongsok Tom Soh,* and Lei Zheng

Cite This: J. Am. Chem. Soc. 2020, 142, 11743−11749

ABSTRACT: Folding energy (ΔG_{fold}) offers a useful metric for characterizing the stability and function of aptamers. However, experimentally measuring the folding energy is challenging, and there is currently no general technique to measure this parameter directly. In this work, we present a simple approach for measuring aptamer folding energy. First, the aptamer is stretched under equilibrium conditions with a double-stranded DNA "molecular clamp" that is coupled to the aptamer ends. We then measure the total internal energy of stressed DNA molecules using time-lapse gel electrophoresis and compare the folding and unfolding behavior of molecular clamp-stressed molecules that incorporate either the aptamer or unstructured random single-stranded DNA in order to derive the aptamer folding energy. Using this approach, we measured a folding energy of 10.40 kJ/mol for the HD22 thrombin aptamer, which is consistent with other predictions and estimates. We also analyzed a simple hairpin structure, generating a folding energy result of 9.05 kJ/mol, consistent with the value predicted by computational models (9.24 kJ/mol). We believe our strategy offers an accessible and generalizable approach for obtaining such measurements with virtually any aptamer.

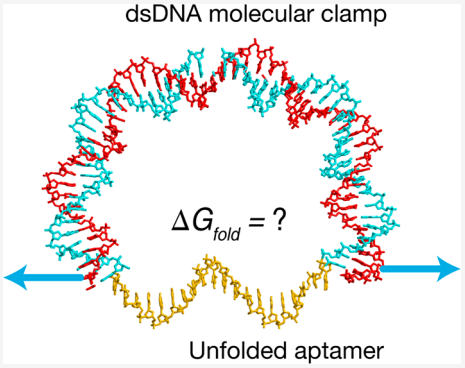

INTRODUCTION

Aptamers offer the powerful capability to recognize and specifically bind to a wide range of biomolecules, including small molecules,[1] metal ions,[2] proteins,[3] and even whole cells.[4] An aptamer's function is dependent upon its capacity to fold into and maintain a binding-competent conformation.[5] As such, the folding energy (ΔG_{fold}) for a given DNA or RNA sequence is an important determinant of aptamer stability, which in turn affects that aptamer's target affinity and specificity, and thus its broader utility in molecular detection and other assays.

Unfortunately, it currently remains difficult to evaluate this parameter because of the difficulties associated with direct measurement of aptamer folding energy at equilibrium. One approach is based on time-dependent single-molecule pulling experiments, in which oligonucleotides are stretched by atomic force microscopy (AFM) or optical tweezers.[6−9] These experiments drive the system away from equilibrium, where the magnitude of the rupture force is related to the pulling rate. As a consequence, one must use the relationship between free energies and irreversible work[10−12] described by Jarzynski's equality[13] to calculate free energy from repeated measurements. However, some have challenged the validity of this approach, arguing that its underlying assumption, i.e., the connection between the microscopic work performed by a time-dependent force with the corresponding Hamiltonian, is theoretically inconsistent.[14−16] Other groups have used ultraviolet spectroscopy or circular dichroism (CD) to generate indirect measurements of melting curves based on distinct differences in the spectroscopic properties of folded and unfolded aptamers.[17,18] However, the arbitrary determination of melting curve baselines can introduce considerable uncertainty, and the assumption that denaturation is only a two-state process with zero heat-capacity change greatly limits the universal application of this approach.[19,20] Others have also performed melting experiments using differential scanning calorimetry (DSC),[18,20] which measures differential heat capacity as a function of temperature.[19,20] However, the accuracy of this approach is not guaranteed, because the ability to correctly determine the values of many thermodynamic parameters is heavily dependent on the choice of appropriate melting models.[20,21]

We describe here a general strategy for directly measuring aptamer folding energy, which eliminates these confounders and sources of bias that can lead to inaccurate measurement. Our method employs a short piece of double-stranded (ds) DNA, which is shorter than the dsDNA persistence length of ∼50 nm, as a "molecular clamp" to pull an aptamer into an unfolded state under equilibrium conditions. Once the appropriate length of the molecular clamp required for successful extension of the aptamer has been determined, we measure the total energy of the constrained molecule—including the bending energy of the molecular clamp and

Received: February 12, 2020
Published: June 3, 2020

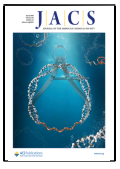

https://dx.doi.org/10.1021/jacs.0c01570
J. Am. Chem. Soc. 2020, 142, 11743−11749

stretching energy of the aptamer—through a simple time-lapse gel electrophoresis method. The folding energy is calculated by comparing against the gel profile of a randomized, unstructured single-stranded (ss) DNA molecule that has been incubated with the same molecular clamp. Here, we demonstrate this method to determine the folding energy of the thrombin aptamer HD22,[22] and derive a measurement that is consistent with prior estimates. Our "folding energy measurement by molecular clamping" (FE-MC) method only requires standard gel electrophoresis equipment and reagents and therefore offers a simple and broadly accessible solution for characterizing aptamer folding and stability.

RESULTS AND DISCUSSION

Overview of the FE-MC Method. The central idea behind the FE-MC method is to exploit short stretches of dsDNA that act as "molecular clamps" to unfold aptamers. This requires the design of two DNA oligonucleotides: strand A contains the aptamer sequence at the center and is flanked by sequences that are complementary to strand B (Figure 1A, left). Therefore, hybridization between strands A and B produces a circularized, partially double-stranded molecule (Figure 1A, right). This structure can be viewed as two coupled (nonlinear) springs, representing the dsDNA and ssDNA component, which are constrained at the same end-to-end distance (EED) x. This represents the distance between the two ends of the molecule after either bending for the dsDNA or stretching for the ssDNA, and describes the degree of deformation for both components. We have termed this circularized molecule a "stressed aptamer molecule" (SAM), with a high internal energy that is stored in the bending energy of the dsDNA component (E_d) and the stretching energy of the ssDNA component (E_s). The dsDNA component applies stretching force at pico-Newton (pN) scales on the ssDNA component (i.e., the aptamer sequence) at equilibrium,[23,24] the stretching behavior of which is modeled as shown in Figure S2A. Since shorter molecular clamps would be expected to exert a stronger extending force (as explained in the Supporting Information, SI), the aptamer may be successfully stretched into an unfolded state (Figure 1A, lower right) or remain folded (Figure 1A, upper right) depending on which state has lower internal energy for varying length of the dsDNA component (N_d), as illustrated in Figure S2B.

The next step entails identification of the appropriate N_d value to ensure that the aptamer is fully extended upon hybridization. To achieve this, we construct a series of SAMs with molecular clamps of varying N_d and subject these constructs to gel electrophoresis. The resulting gel will show multiple bands corresponding to monomers, dimers, and other multimers arising from polymerization of multiple copies of strand A and strand B. In this step, we need to identify the value of N_d at which splitting of the monomer band is observed (Figure 1B), indicating the coexistence of two possible configurations with similar internal energy (as depicted in Figure S3). This represents the transition length (N_c) of the molecular clamp: when $N_d < N_c$, the aptamer is stretched and unfolded, whereas when $N_d > N_c$, the aptamer remains in a folded state.

We then select a SAM for which the molecular clamp length N_d is smaller than N_c for further analysis. It is important to note that there is a break in the middle of the dsDNA component of the SAM, which arises from the two ends of the aptamer-flanking "arms" of strand A after hybridization with

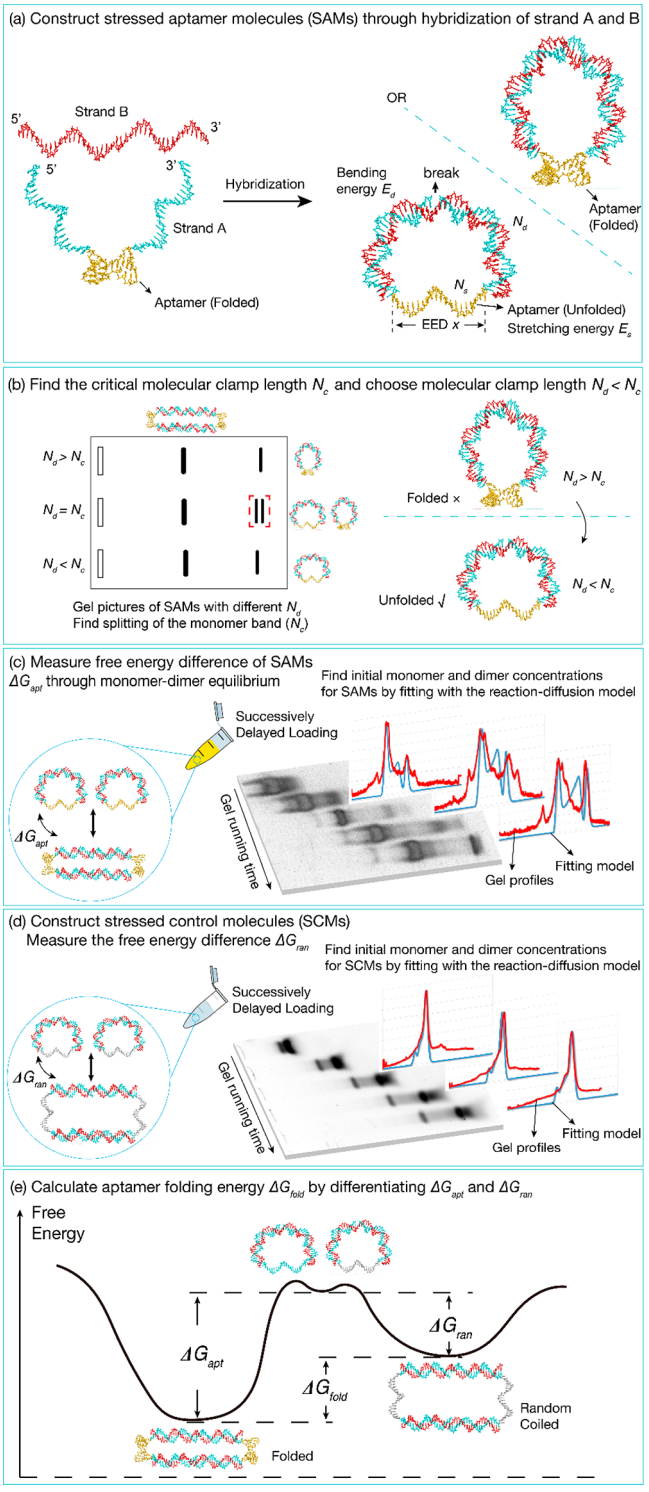

Figure 1. Determination of aptamer folding energy using the molecular clamp (FE-MC) method. (A) We construct a series of stressed aptamer molecules (SAMs) through hybridization of strand A, which contains the aptamer sequence of interest (yellow), and strand B. The aptamer may be unfolded (upper right) or remain folded (lower right) depending on dsDNA length (N_d). (B) Gel electrophoresis of SAMs with different N_d values to find the critical molecular clamp length (N_c), identified as the SAM in which splitting of the monomer band is observed (red dashed box). A SAM in which $N_d < N_c$ is chosen for subsequent steps. (C) Quantification of the internal energy (ΔG_{apt}) of the chosen SAM using eq 1, in which we measure the equilibrium monomer and dimer concentrations by fitting "snapshots" of time-lapse gel profiles (red curves) with the

https://dx.doi.org/10.1021/jacs.0c01570
J. Am. Chem. Soc. 2020, 142, 11743−11749

Figure 1. continued

reaction-diffusion model (blue curves). (D) We next construct stressed control molecules (SCMs), in which the aptamer from the SAM is substituted with an unstructured randomized sequence, and measure the SCM internal energy (ΔG_{ran}). (E) The energy levels occupied by the monomeric and dimeric states of the SAM and SCM. The energy level is the same for the unfolded SAM and SCM monomers, but the dimer energy levels are different. The aptamer folding energy ΔG_{fold} is calculated as $\Delta G_{apt} - \Delta G_{ran}$.

strand B. This break means that the SAM may relax its internal elastic energy through the formation of multimers, in which the dsDNA component is not forced to bend and the ssDNA component is not subject to stretching.[25] Because polymerization lowers the entropy of molecules, there exists a chemical equilibrium of monomer−dimer interconversion, which can be observed through gel electrophoresis, with multiple bands corresponding to dimers and other multimers (Figure 1C).

Quantitatively, this monomer−dimer interconversion can be described in terms of the equality of monomer and dimer chemical potentials, namely $2\mu_M = 2\Delta G_{M-1/2D} + 2k_BT \ln X_M$ and $\mu_D = k_BT \ln X_D$. The internal energy of the SAM is hence described by the following equation:

$$\Delta G_{M-1/2D} = \frac{1}{2}k_BT\ln\left(\frac{X_D}{X_M^2}\right) = \frac{1}{2}k_BT\ln\left[\frac{C_D/C_W}{(C_M/C_W)^2}\right] \quad (1)$$

where X_D and X_M are the molar fractions and C_D and C_M are the concentrations of the monomer and dimer, respectively. C_W = 55 M is the concentration of water (see the Methods section for derivation details). Equation 1 suggests that the internal energy of the SAM can simply be computed by quantification of monomer and dimer populations at equilibrium (e.g., through gel electrophoresis). It is worth noting that this monomer−dimer interconversion continues even during gel electrophoresis, leading to bias in monomer and dimer concentrations relative to initial equilibrium values. To address this problem, we have adopted a "time-lapse" gel electrophoresis method (Figure 1C, right). Specifically, multiple aliquots of the same chosen SAM sample (in which $N_d < N_c$) are loaded into different lanes at successive times. The gel image for this SAM is then collected to show the evolution of monomer and dimer bands with time, enabling extrapolation back to initial equilibrium concentrations. A reaction-diffusion model is applied with the initial monomer and dimer concentrations as fitting parameters, and their values are determined so that the gel profiles at each running time are fitted to model curves with the same set of parameters (Figure 1C, right; see the Methods section for details). The initial concentrations are then plugged into eq 1 to calculate the internal energy ΔG_{apt} within the SAM.

Next, we construct stressed control molecules (SCMs), in which the aptamer sequence in strand A has been replaced with a randomized sequence (Figure 1D). We extract the internal energy within the SCM (ΔG_{ran}) in the same way as for the SAM. Finally, we compute the aptamer folding energy as follows: $\Delta G_{fold} = \Delta G_{apt} - \Delta G_{ran}$ (Figure 1E). Since the aptamers in the SAM dimers are in a folded state while the randomized sequences in the SCM dimers are in a random-coiled state, $\Delta G_{apt} - \Delta G_{ran}$ cancels the contribution of base-pairing in half of the SAM and SCM dimers, and yields the energy difference between the folded aptamer and the random DNA coil (see the SI).

Although the hybridization of the dsDNA component was checked using the DINAMelt web server to minimize the likelihood of "slipping" effects (i.e., alternative, non-Watson−Crick base-pairings), such slipping events may still occur in the final assay due to the high bending energy when using dsDNA as a molecular clamp. However, this does not affect the final measured free energy value. This is because the free energy computed using eq 1 actually represents the energy difference between one monomer and a half dimer, in which dsDNA is not constrained to bend. Monomers with slipping base-pairs are in the same high-energy "excited states", because the free energy penalty of base-pair slipping eventually compensates for the released bending energy.

Folding Energy Measurement of the HD22 Thrombin Aptamer. To demonstrate the FE-MC method, we chose an aptamer that recognizes human α-thrombin (HD22).[22] This 29-nt aptamer (5′-AGTCCGTGGTAGGG-CAGGTTGGGGTGACT-3′) contains a duplex/G-quadruplex mixed structure[26] and exhibits strong target affinity ($K_D \approx$ 0.5 nM). We constructed a series of HD22 SAMs with N_d ranging from 18−24 bp. Time-lapse gel images of these SAMs are shown in Figure 2. When N_d = 20 bp, splitting of the monomer bands was observed (Figure 2B), indicating that this was the N_c of the molecular clamp; when $N_d < 20$, the HD22 aptamer was unfolded, whereas when $N_d > 20$, the HD22 aptamer remained in the folded state.

We selected an unfolded SAM (N_d = 18 bp; SAM18) for subsequent detailed analysis. A time-lapse gel image of SAM18

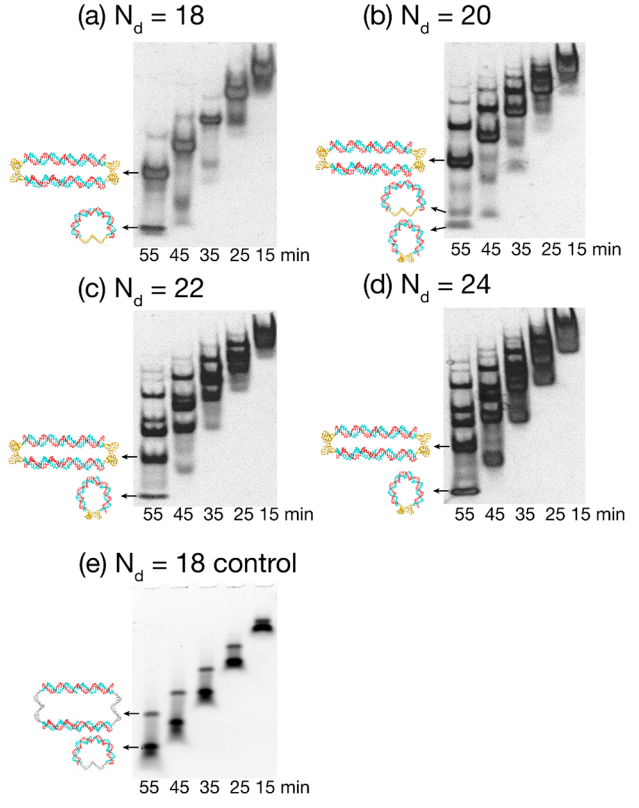

Figure 2. Time-lapse gel images for SAMs with the HD22 aptamer and N_d = 18 (A), 20 (B), 22 (C), and 24 bp (D). (E) Time-lapse gel pictures for an SCM with a randomized control sequence and N_d = 18.

https://dx.doi.org/10.1021/jacs.0c01570
J. Am. Chem. Soc. 2020, 142, 11743−11749

was collected as shown in Figure 2A and the gel profiles in different lanes (i.e., at different running times) were successfully fitted with the reaction-diffusion model (Figure S4A, see the SI for fitting details). We found that the initial equilibrium concentrations of monomer and dimer were 0.42 and 0.79 μM, respectively. We hence calculated the internal energy of the SAM18 monomer

$$\Delta G_{\mathrm{SAM18}} = \frac{1}{2}k_{\mathrm{B}}T \ln\left[\frac{0.79\ \mu\mathrm{M}/55\ \mathrm{M}}{(0.42\ \mu\mathrm{M}/55\mathrm{M})^2}\right] = 9.96k_{\mathrm{B}}T = G^{\mathrm{SAM18}}_{\mathrm{Monomer}} - \frac{1}{2}G^{\mathrm{SAM18}}_{\mathrm{dimer}}$$

using eq 1. This describes the free energy difference between the SAM18 monomer ($G^{\mathrm{SAM18}}_{\mathrm{Monomer}}$) and half of the SAM18 dimer ($1/2G^{\mathrm{SAM18}}_{\mathrm{Dimer}}$).

We next constructed SCM18, with the same molecular clamp, but where strand A incorporated a control 29-mer randomized sequence (5′-CAGCAGGCAATCGATACACA-CACAGTAGA-3′) with no secondary structure (checked by the DINAMelt web server[27]). The time-lapse gel image was collected as shown in Figure 2E. The internal molecular energy was calculated using eq 1 by fitting the SCM18 gel profiles with the reaction-diffusion model (Figure S4B). We found that the initial monomer and dimer concentrations for the SCM were 1.78 and 0.11 μM, respectively (see the SI for fitting details). Thus, $\Delta G_{\mathrm{SCM18}} = 5.62k_{\mathrm{B}}T = \Delta G^{\mathrm{SCM18}}_{\mathrm{Monomer}} - 1/2G^{\mathrm{SCM18}}_{\mathrm{Dimer}}$.

SAM18 and SCM18 shared the same free energy in their stretched state, but the aptamers in the SAM18 dimers were folded while the randomized sequences in the SCM18 dimers were in a random-coiled state, leading to a difference in energy levels. Accordingly, the differential between ΔG_{SAM18} and ΔG_{SCM18} canceled the base-pairing energy in half of the SAM and SCM dimers, yielding the energy difference between the folded aptamer and the random DNA coil. Specifically, this can be calculated as follows:

$$\Delta G_{\mathrm{SAM18}} - \Delta G_{\mathrm{SCM18}} = \frac{1}{2}G^{\mathrm{SCM18}}_{\mathrm{dimer}} - \frac{1}{2}G^{\mathrm{SAM18}}_{\mathrm{dimer}} = \Delta G^{\mathrm{HD22}}_{\mathrm{fold}} = 4.34k_{\mathrm{B}}T$$

or 10.40 kJ/mol for the HD22 folding energy.

Validation of the Experimental Results. In order to validate this measurement, we calculated the critical molecular clamp length (N_c) to check whether it was consistent with experimental observations. The theoretical value of N_c was determined for a scenario in which the folded and extended states of the SAM have similar energy values. Our determination of the folding energy for HD22 (4.34 $k_{\mathrm{B}}T$) was plugged into the model of the aptamer folding energy profile (see the SI) as the ssDNA stretching energy of the SAM. The EED x between the two ends of the SAM was used to characterize the degree of deformation for the two SAM components. The total energy (E_{tot}) of the SAM as a function of the EED x was calculated using the sum of the ssDNA stretching energy and dsDNA bending energy (see the SI). We found that when N_d = 20, the local energy minimum of the folded state was 4.95 $k_{\mathrm{B}}T$, while that of the stretched state was 5.20 $k_{\mathrm{B}}T$, as shown in Figure S3. The similarity of the two energy values indicates that N_d = 20 is the theoretical critical length, consistent with our experimental results.

We also compared the final HD22 folding energy value 4.34 $k_{\mathrm{B}}T$ (or 10.40 kJ/mol) to other estimates. Prior studies of aptamer folding based on pulling experiments using AFM or optical tweezers have yielded free energy estimates for the complete unfolding of the *pbuE* riboswitch aptamer in the range of 2−3 kcal/mol (8.4−12.6 kJ/mol),[9] the same order of magnitude for energy scale as we obtained with HD22 using our orthogonal method. For this particular aptamer, the DINAMelt web server[27] predicts a folding energy of just 1.11 kcal/mol (4.67 kJ/mol), which is much smaller than the value we obtained. This is because the DINAMelt algorithm does not account for the energy of the 3D structure of the G-quadruplex. According to previous studies using UV-spec or DSC, the ultimate free energy ΔG(310 K) for a low-order G-quadruplex is approximately 1.50 kcal/mol (6.30 kJ/mol).[17,19] Since HD22 features a combination of duplex and G-quadruplex structure,[26] a rough estimate from adding the base-pairing energy of the duplex (4.67 kJ/mol) and the G-quadruplex folding energy (6.30 kJ/mol) yields a total folding energy of 10.97 kJ/mol for HD22, which is very similar to the value we calculated (10.40 kJ/mol).

Such an estimate is necessary given the lack of directly comparable, precise folding energy predictions by other metrics, but we were also able to confirm the accuracy of our FE-MC approach with a simple hairpin structure (5′-TTGTCAT TTTTTTTTTTTTTTTATGACTT-3′). The folding energy of this simple structure is easily predicted by DINAMelt[27] to be 9.24 kJ/mol under ambient conditions, and FE-MC yielded a highly consistent measurement of 9.05 kJ/mol (see the SI for details), further supporting the validity and accuracy of our approach.

4. CONCLUSION

In this work, we describe a simple approach for probing the folding energy of aptamers. In our ME-FC method, the aptamer is unfolded by a dsDNA component that acts as a molecular clamp under equilibrium conditions. The internal energy of this stressed aptamer molecule is determined using time-lapse gel electrophoresis and then compared against a similar stressed DNA molecule in which the aptamer has been substituted with a randomized ssDNA with no secondary structure. The internal energy difference between the two stressed molecules yields the aptamer folding energy.

Using this approach with the HD22 thrombin aptamer as a model, we computed a folding energy of 4.34 $k_{\mathrm{B}}T$ (~10.4 kJ/mol), which is in keeping with aptamer folding energy scales from other studies as well as rough predictions based on HD22's structure. We also validated the accuracy of FE-MC by correctly measuring the folding energy of a hairpin structure, obtaining results that mirror the value predicted by the DINAMelt web server. Although we have calculated the folding energy measurement of a relatively short aptamer (29 nt) here, the FE-MC method should also be applicable to aptamers with longer lengths of 60−80 nt. This is valuable in that many newly selected aptamers include primer-biding sites and have not been minimized. The applicable upper limit of our dsDNA molecular clamp is roughly 10.0 $k_{\mathrm{B}}T$ (~24.0 kJ/mol) based on dsDNA bending energy (Figure S1), which is already adequate for most DNA/RNA folding structures. It

https://dx.doi.org/10.1021/jacs.0c01570
J. Am. Chem. Soc. 2020, 142, 11743−11749

Table 1. DNA Sequences Used to Form SAMs with Different N_d

	Strand A (5' to 3')	*Strand B (5' to 3')*
Group 1 (N_d = 24)	ACG TGA GAG CAG AGTCCGTGGTAGGGCAGGTTGGGGTG ACT GAC ATA CGA CGA	CTG CTC TCA CGT TCG TCG TAT GTC
Group 2 (N_d = 22)	ACG TGA GAG CA AGTCCGTGGTAGGGCAGGTTGGGGTG ACT AC ATA CGA CGA	TG CTC TCA CGT TCG TCG TAT GT
Group 3 (N_d = 20)	ACG TGA GAG C AGTCCGTGGTAGGGCAGGTTGGGGTG ACT C ATA CGA CGA	G CTC TCA CGT TCG TCG TAT G
Group 4 (N_d = 18)	ACG TGA GAG AGTCCGTGGTAGGGCAGGTTGGGGTG ACT ATA CGA CGA	CTC TCA CGT TCG TCG TAT

should be feasible to further extend this energy range by using "stiffer" artificial DNA backbones for the molecular clamp, such as peptide nucleic acids (PNAs) and xeno nucleic acids (XNAs). The folding energy scale of protein complexes and DNA/protein interfaces may be beyond this range, but dsDNA molecular clamps have also been applied to perturb the excited states of enzymes for manual control of their activity.[28,29] Since FE-MC only requires time-lapse gel electrophoresis experiments, we believe it offers a highly accessible and generalizable method for evaluating aptamers in a simple and direct manner.

METHODS AND MATERIALS

Sample Preparation. All oligonucleotide sequences (listed in Table 1) were synthesized by Sangon Biotech (Shanghai) with HPLC purification. The sequences shown in red for strand A hybridize with the corresponding strand B. The red sequence of Group 1 was randomly generated with 60% GC content and then shortened by two bases progressively for Groups 2 to 4, as shown in Table 1. The thermodynamic properties of the sequences were carefully analyzed using the DINAMelt web server[27,30] to ensure successful hybridization of dsDNA while minimizing slipping effects (i.e., high energy for alternative, non-Watson−Crick base pairings).

Each strand A was mixed with equimolar amounts of strand B and diluted to a final concentration of 2 μM and a final volume of 200 μL in the hybridizing buffer (10 mM Tris, 5 mM $MgCl_2$, 100 mM NaCl, pH 7.9). The mixture was then heated at 95 °C for 10 min and annealed at room temperature overnight (~0.065 °C/min) to ensure the proper conformational structures in stressed DNA molecules.

Once an appropriate length of dsDNA molecular clamp for the SAM was determined, stressed control molecules (SCMs) were constructed by replacing the aptamer from the SAMs (i.e., the black sequence in Table 1) with a randomized ssDNA of the same length. The thermodynamics of the randomized ssDNA were checked using the DINAMelt web server[27,30] so that there was no secondary structure in the ssDNA. For the HD22 folding energy measurement, the randomized sequence CAG CAG GCA ATC GAT ACA CAC CAG TAG AC was chosen.

Molecular Energy Extraction Based on Monomer−Dimer Equilibrium. At equilibrium of monomer−dimer interconversion, the chemical potentials for two monomers ($2\mu_M = 2\Delta G_{M-1/2D} + 2k_BT \ln X_M$) and one dimer ($\mu_D = k_BT \ln X_D$) are equal: $2\Delta G_{M-1/2D} + 2k_BT \ln X_M = k_BT \ln X_D$. Since the base-pairing is identical for one dimer and two monomers, the energetic contribution of base-pairing cancels out and the internal elastic energy stored in the monomer can be characterized by the following equation:[25]

$$\Delta G_{M-1/2D} = \frac{1}{2} k_B T \ln\left(\frac{X_D}{X_M^2}\right)$$

where $X_D = C_D/C_W$ and $X_M = C_M/C_W$, describing the molar fraction of the monomer and dimer, respectively, and C_M and C_D are the respective concentrations of the two species. C_W = 55 M is the concentration of water. This equation essentially gives the energy difference between the monomer and half of the dimer (as the ground state), and suggests that this energy difference can be simply extracted by measuring the equilibrium monomer and dimer concentrations.

Time-Lapse Gel Electrophoresis. Concentrations of monomers and dimers were experimentally determined by time-lapse gel electrophoresis with a 5% polyacrylamide gel, based on the intensities of the corresponding gel bands (using necessary calibrations as described in ref 25). The monomer−dimer interconversion of the stressed DNA molecules also occurs while the sample is moving through the gel and has to be taken into account. Therefore, in order to extrapolate back the initial equilibrium concentrations of the population of monomers and dimers at t_0, we loaded different lanes of the gel with aliquots from the same sample at intervals of 10 min to capture "snapshot" gel profiles at different times. These various aliquots were run under 100 V for 55, 45, 35, 25, and 15 min, respectively. Images from time-lapse gel electrophoresis were converted to gel profiles using ImageJ ver1.51.

Reaction-Diffusion Model. In order to extract the initial population of monomers and dimers, we fitted these gel profiles with a reaction-diffusion model[31] that has been successfully applied to the analysis of electrophoresis with protein−DNA,[32] hairpin-duplex,[33] and monomer−dimer[23,25] interconversions. The model formulas are

$$\frac{\partial C_m}{\partial t} = D_m \frac{\partial^2 C_m}{\partial x^2} - V_m \frac{\partial C_m}{\partial x} - 2k_1 C_m^2 + 2k_2 C_d$$

$$\frac{\partial C_d}{\partial t} = D_d \frac{\partial^2 C_d}{\partial x^2} - V_d \frac{\partial C_d}{\partial x} + k_1 C_m^2 - k_2 C_d$$

where C_m and C_d are the concentration of monomers and dimers, respectively, as a function of gel running time t and gel vertical position x from the bottom of the loading well, D_m and D_d are the diffusion constants of the two species, V_m and V_d are their mobilities, k_1 is the conversion rate from monomers to dimers, and k_2 is the rate for the reverse reaction. During fitting with the reaction-diffusion model, V_m and V_d were first determined by measuring the distance that the population had shifted at various running times. D_m and D_d were determined from the width of the corresponding peaks of monomers and dimers. The initial monomer and dimer concentrations (C_{m0} and C_{d0}) and interconversion rates (k_1 and k_2) were adjusted so that the model could fit the gel profiles at different times (i.e., in different lanes) with the same set of parameters. Finally, C_{m0}

https://dx.doi.org/10.1021/jacs.0c01570
J. Am. Chem. Soc. 2020, 142, 11743−11749

and C_{d0} were used to calculate the internal energy of the stressed DNA molecules.

Note that the computed elastic energy was rather insensitive to the parameter values in the model. Even a barely fair fitting to the gel profiles, in which the interconversion rates were set to zero, leads to a difference of ∼15% in the initial concentration values, which in turn resulted in only a ∼0.2 k_BT change in the final elastic energy result due to the logarithmic function in eq 1.

■ ASSOCIATED CONTENT

Supporting Information

The Supporting Information is available free of charge at https://pubs.acs.org/doi/10.1021/jacs.0c01570.

Mechanics of dsDNA as molecular clamp; model of aptamer folding energy profile; the effect of molecular clamps on aptamer folding states; comparison of the experimental results with a theoretical model; fitting details using the reaction-diffusion model; and demonstration of the FE-MC method with hairpin structures (PDF)

■ AUTHOR INFORMATION

Corresponding Authors

Hao Qu − *School of Food and Biological Engineering, Hefei University of Technology, Hefei 230009, China;* Email: quhao@hfut.edu.cn

Hyongsok Tom Soh − *Department of Electrical Engineering and Department of Radiology, Stanford University, Stanford, California 94305, United States;* orcid.org/0000-0001-9443-857X; Email: tsoh@stanford.edu

Authors

Qihui Ma − *School of Food and Biological Engineering, Hefei University of Technology, Hefei 230009, China*

Lu Wang − *School of Food and Biological Engineering, Hefei University of Technology, Hefei 230009, China*

Yu Mao − *School of Food and Biological Engineering, Hefei University of Technology, Hefei 230009, China*

Michael Eisenstein − *Department of Electrical Engineering and Department of Radiology, Stanford University, Stanford, California 94305, United States*

Lei Zheng − *School of Food and Biological Engineering, Hefei University of Technology, Hefei 230009, China;* orcid.org/0000-0001-8367-5502

Complete contact information is available at: https://pubs.acs.org/10.1021/jacs.0c01570

Notes

The authors declare no competing financial interest.

■ ACKNOWLEDGMENTS

This study was supported by the National Key R&D Program of China (2017YFC1600603), the National Natural Science Foundation of China (21705031), the Natural Science Foundation of Anhui Province (1808085QB39), the Fundamental Research Funds for the Central Universities (PA2019GDQT0018), and Engineering Research Center of Bioprocess by Ministry of Education in Hefei University of Technology. This work was also supported by the Chan-Zuckerberg Biohub (HTS).

■ REFERENCES

(1) McKeague, M.; DeRosa, M. C. Challenges and Opportunities for Small Molecule Aptamer Development. *J. Nucleic Acids* **2012**, *2012*, 1.

(2) Qu, H.; Csordas, A. T.; Wang, J.; Oh, S. S.; Eisenstein, M. S.; Soh, H. T. Rapid and Label-Free Strategy to Isolate Aptamers for Metal Ions. *ACS Nano* **2016**, *10* (8), 7558−7565.

(3) Keefe, A. D.; Pai, S.; Ellington, A. Aptamers as Therapeutics. *Nat. Rev. Drug Discovery* **2010**, *9*, 537.

(4) Fang, X.; Tan, W. Aptamers Generated from Cell-SELEX for Molecular Medicine: A Chemical Biology Approach. *Acc. Chem. Res.* **2010**, *43* (1), 48−57.

(5) Long, S. B.; Long, M. B.; White, R. R.; Sullenger, B. A. Crystal Structure of an RNA Aptamer Bound to Thrombin. *RNA* **2008**, *14* (12), 2504−2512.

(6) Wang, M. D.; Yin, H.; Landick, R.; Gelles, J.; Block, S. M. Stretching DNA with Optical Tweezers. *Biophys. J.* **1997**, *72* (3), 1335−1346.

(7) Woodside, M. T.; García-García, C.; Block, S. M. Folding and Unfolding Single RNA Molecules under Tension. *Curr. Opin. Chem. Biol.* **2008**, *12* (6), 640−646.

(8) Bustamante, C.; Bryant, Z.; Smith, S. B. Ten Years of Tension: Single-Molecule DNA Mechanics. *Nature* **2003**, *421*, 423.

(9) Greenleaf, W. J.; Frieda, K. L.; Foster, D. A. N.; Woodside, M. T.; Block, S. M. Direct Observation of Hierarchical Folding in Single Riboswitch Aptamers. *Science* **2008**, *319* (5863), 630−633.

(10) Hummer, G.; Szabo, A. Free Energy Reconstruction from Nonequilibrium Single-Molecule Pulling Experiments. *Proc. Natl. Acad. Sci. U. S. A.* **2001**, *98* (7), 3658.

(11) Hummer, G.; Szabo, A. Free Energy Profiles from Single-Molecule Pulling Experiments. *Proc. Natl. Acad. Sci. U. S. A.* **2010**, *107* (50), 21441.

(12) Ciliberto, S. Experiments in Stochastic Thermodynamics: Short History and Perspectives. *Phys. Rev. X* **2017**, *7* (2), 021051.

(13) Jarzynski, C. Nonequilibrium Equality for Free Energy Differences. *Phys. Rev. Lett.* **1997**, *78* (14), 2690−2693.

(14) Gore, J.; Ritort, F.; Bustamante, C. Bias and Error in Estimates of Equilibrium Free-Energy Differences from Nonequilibrium Measurements. *Proc. Natl. Acad. Sci. U. S. A.* **2003**, *100* (22), 12564.

(15) Cohen, E. G. D.; Mauzerall, D. A Note on the Jarzynski Equality. *J. Stat. Mech.: Theory Exp.* **2004**, *2004* (07), P07006.

(16) Vilar, J. M. G.; Rubi, J. M. Failure of the Work-Hamiltonian Connection for Free-Energy Calculations. *Phys. Rev. Lett.* **2008**, *100* (2), 020601.

(17) Mergny, J.-L.; Phan, A.-T.; Lacroix, L. Following G-Quartet Formation by UV-Spectroscopy. *FEBS Lett.* **1998**, *435* (1), 74−78.

(18) Bončina, M.; Lah, J.; Prislan, I.; Vesnaver, G. Energetic Basis of Human Telomeric DNA Folding into G-Quadruplex Structures. *J. Am. Chem. Soc.* **2012**, *134* (23), 9657−9663.

(19) Lane, A. N.; Chaires, J. B.; Gray, R. D.; Trent, J. O. Stability and Kinetics of G-Quadruplex Structures. *Nucleic Acids Res.* **2008**, *36* (17), 5482−5515.

(20) Haq, I.; Chowdhry, B. Z.; Jenkins, T. C. Calorimetric Techniques in the Study of High-Order DNA-Drug Interactions. In *Methods in Enzymology*; Academic Press: New York, 2001; Vol. *340*, pp 109−149.

(21) Spink, C. H. Differential Scanning Calorimetry. In *Methods in Cell Biology*; Academic Press: New York, 2008; Vol. *84*, pp 115−141.

(22) Tasset, D. M.; Kubik, M. F.; Steiner, W. Oligonucleotide Inhibitors of Human Thrombin that Bind Distinct Epitopes. *J. Mol. Biol.* **1997**, *272* (5), 688−698.

(23) Qu, H.; Zocchi, G. The Complete Bending Energy Function for Nicked DNA. *EPL (Europhysics Letters)* **2011**, *94* (1), 18003.

(24) Qu, H.; Wang, Y.; Tseng, C.-Y.; Zocchi, G. Critical Torque for Kink Formation in Double-Stranded DNA. *Phys. Rev. X* **2011**, *1* (2), 021008.

(25) Qu, H.; Tseng, C.-Y.; Wang, Y.; Levine, A. J.; Zocchi, G. The Elastic Energy of Sharply Bent Nicked DNA. *EPL (Europhysics Letters)* **2010**, *90* (1), 18003.

(26) Russo Krauss, I.; Pica, A.; Merlino, A.; Mazzarella, L.; Sica, F. Duplex-Quadruplex Motifs in a Peculiar Structural Organization Cooperatively Contribute to Thrombin Binding of a DNA Aptamer. *Acta Crystallogr., Sect. D: Biol. Crystallogr.* **2013**, *69* (12), 2403−2411.
(27) Markham, N. R.; Zuker, M. DINAMelt Web Server for Nucleic Acid Melting Prediction. *Nucleic Acids Res.* **2005**, *33*, W577−W581.
(28) Choi, B.; Zocchi, G.; Wu, Y.; Chan, S.; Jeanne Perry, L. Allosteric Control through Mechanical Tension. *Phys. Rev. Lett.* **2005**, *95* (7), 078102.
(29) Tseng, C.-Y.; Zocchi, G. Mechanical Control of Renilla Luciferase. *J. Am. Chem. Soc.* **2013**, *135* (32), 11879−11886.
(30) Owczarzy, R.; Tataurov, A. V.; Wu, Y.; Manthey, J. A.; McQuisten, K. A.; Almabrazi, H. G.; Pedersen, K. F.; Lin, Y.; Garretson, J.; McEntaggart, N. O.; Sailor, C. A.; Dawson, R. B.; Peek, A. S. IDT SciTools: A Suite for Analysis and Design of Nucleic Acid Oligomers. *Nucleic Acids Res.* **2008**, *36*, W163−W169.
(31) Shunong, Y.; Wolska-Klis, M. M.; Cann, J. R. Gel Electrophoresis of Reacting Macromolecules. Rate-Limited Self-Association. *Anal. Biochem.* **1991**, *196* (1), 192−198.
(32) Cann, J. R. Theoretical Studies on the Mobility-Shift Behavior of Binary Protein-DNA Complexes. *Electrophoresis* **1993**, *14* (1), 669−679.
(33) Shubsda, M.; Goodisman, J.; Dabrowiak, J. C. Characterization of Hairpin-Duplex Interconversion of DNA Using Polyacrylamide Gel Electrophoresis. *Biophys. Chem.* **1999**, *76* (2), 95−115.

https://dx.doi.org/10.1021/jacs.0c01570
J. Am. Chem. Soc. 2020, 142, 11743−11749